PASJ: Publ. Astron. Soc. Japan , –6 (2008)

The Radio-to-Submillimeter Flux Density Ratio of Galaxies as a Measure of Redshift

T. N. Rengarajan and Tsutomu T. Takeuchi
Division of Particle and Astrophysical Sciences, School of Science, Nagoya University,
Furo-cho, Chikusa-ku, Nagoya 464–8602
renga, takeuchi@u.phys.nagoya-u.ac.jp

(Received 2000 December 26; accepted 2001 April 20)

Abstract

We re-examine the technique of determining the redshifts of galaxies from the ratio of the submillimeter-to-radio continuum flux densities based on a recently published catalog of 850 μm sources. We derived the expected variation of this ratio as a function of redshift incorporating the expected average luminosity and the spectral energy distribution (SED) of dust emission and the radio continuum. We find that the existing data for most of the high redshift ($z \gtrsim 1$) sources correspond to our new calculation. Amongst the well-identified sources, there is none with an index significantly higher than predicted. Sources which have an index lower than predicted are either within the error zone or much lower, the latter presumably having AGN-dominated radio-continuum emission. We find the median redshift to be ~ 2, which is consistent with that deduced by previous work (~ 3) within the error. We also discuss the various systematic effects that can affect the accuracy of the redshift estimate. We examine other methods of redshift estimation, like photometric ratio in the submillimeter and locating the peak of the SED in the rest system of the objects. We conclude that while the various methods are helpful in identifying high-redshift objects and making a crude estimate of the redshift, they are not, at present, accurate enough for a detailed study of redshift distribution of the submillimeter galaxies.

Key words: galaxies: redshifts — galaxies: starbursts — infrared : galaxies — radio continuum : galaxies

1. Introduction

It was first suggested by Carilli and Yun (1999; hereafter CY) that an estimate of the redshift of distant galaxies can be obtained from the ratio of the submillimeter (submm) to radio continuum flux densities. Following this work, several others have applied this technique to various samples (Smail et al. 2000; Barger et al. 2000). The former make use of a complete sample of 850 μm observations. This method has been used by several authors to obtain the redshift distribution of galaxies detected in the submm wavelengths (Smail et al. 2000; Barger et al. 1999; Bertoldi et al. 2000; Ivison et al. 2000). The basis for this method is the tight correlation between the far infrared (FIR) flux in a broad band of 40–120 μm (defined through the FIR parameter by Helou et al. 1988) and the radio continuum flux density (FD) at cm wavelengths (Condon 1992 and references therein). CY have discussed extensively the advantages of using these wavelengths. The steep nature of the submm SED and the fact that as the redshift increases, the FD at the rest system submm wavelength increases sharply, while the corresponding radio FD decreases give rise to a fast change in the FD ratio with z. The accuracy of the method depends on the extent of the variation of SED from galaxy to galaxy. Once the local value of the submm-to-radio ratio, $\mathcal{R}_{\rm sr} = S(353\ {\rm GHz})/S(1.49\ {\rm GHz})$, and the dust emission SED are known, the $\mathcal{R}_{\rm sr}$–z behavior can be predicted.

Most authors have used a modified blackbody spectrum with an emissivity dependence of $\epsilon(\nu) \propto \nu^n$ with $n = 1$–1.5 and the $\mathcal{R}_{\rm sr}$ value of nearby prototype galaxies, like M 82 or Arp 220, and other ultraluminous galaxies since a good sample of submm local galaxies was not available. Blain (1999a) and Carilli and Yun (2000a) have discussed the uncertainties associated with this method. Though they treated some important issues of real SEDs, many aspects are still overlooked and remain to be considered with regard to a large well-controlled sample of galaxies.

Recently, Dunne et al. (2000, hereafter DS-I) have published a catalog of 850 μm flux densities for a complete sample of 104 bright IRAS galaxies. This large sample can profitably be used to compute the expected variation of $\mathcal{R}_{\rm sr}$ with z. In their erratum (Carilli, Yun 2000b) Carilli and Yun have also commented on the Dunne et

al. data. Therefore, we discuss this method further and compare available observations for well-identified high-z galaxies with our computed curve. We also estimate the dispersion in the relationship and discuss the limitations of the method. Finally, we briefly comment on other methods proposed for a redshift determination, such as those using the submm photometric ratio (Hughes et al. 1998) and those locating the peak of the FIR emission (Blain 1999a, 1999b).

2. Data and Analysis

2.1. Submillimeter Data

Dunne et al. (2000) tabulated the data for a complete sub-sample of IRAS galaxies selected from the Bright Galaxy Sample (Soifer et al. 1989). Besides other information, they tabulated the 850 μm flux densities measured using SCUBA and parameters of fits to the SED using their data and the IRAS 60 and 100 μm FDs. They assumed a modified blackbody spectrum characterized by dust temperature, $T_{\rm d}$ and a dust emissivity index, n. Though these values may not correctly represent the physical temperature, they give a reasonable measure of the SED at wavelengths longer than 60 μm. The mean and dispersion of $T_{\rm d}$ and n are 35.6±4.9 K and 1.3 ± 0.2, respectively. Using the parameter FIR $= 1.26 \times 10^{-14} \times [2.58\,S(60) + S(100)]$ and $H_0 = 75$ Mpc^{-1}km s^{-1} the computed FIR luminosity, $L_{\rm FIR}$, ranges from 10^{10} to 10^{12} $L_\odot$. Radio-continuum FDs at 1.49 GHz are available for almost all DS-I sources from Condon et al. (1990, 1996). Using these along with the DS-I 850 μm data, we find the mean and dispersion of log $\mathcal{R}_{\rm sr}$ to be 0.43 and 0.24, respectively. From a more careful look at the data, it is seen that $log\mathcal{R}_{\rm sr}$ is a decreasing function of $L_{\rm FIR}$, changing from 0.55 in the $\log L_{\rm FIR}/L_\odot$ interval 10–10.3 to 0.29 for the 11.2–12 interval. This result arises mainly due to the correlation between $(T_{\rm d}, n)$ and $L_{\rm FIR}$ affecting the ratio $S(353$ GHz$)$/FIR. We discuss the effect of this later. If a galaxy located at a redshift z is observed at frequencies $\nu_{\rm s}^{\rm obs}$ and $\nu_{\rm r}^{\rm obs}$ at the Earth where the subscripts s and r refer to submm and radio, respectively, the observed ratio is related to the rest system ratio by the relation

$$\mathcal{R}_{\rm sr} = \frac{S(\nu_{\rm s}^{\rm obs})}{S(\nu_{\rm r}^{\rm obs})} = \frac{S[(1+z)\nu_{\rm s}^{\rm em}]}{S[(1+z)\nu_{\rm r}^{\rm em}]}\,. \qquad (1)$$

If the radio SED is a power law of the form, $S(\nu_{\rm r}) \propto \nu_{\rm r}^{\alpha}$, the denominator can be replaced by $(1+z)^{\alpha} S(\nu_{\rm r}^{\rm em})$. For a subsequent discussion, we take $\nu_{\rm s} = 353$ GHz and $\nu_{\rm r} = 1.49$ GHz. For each source of DS-I, we compute $S[353(1+z)]$ using the fitted values of $T_{\rm d}$ and n for that source and take the ratio to the observed 1.49 GHz FD. The mean and dispersion of the ratio are then computed as a function of redshift. What about the effect of a luminosity–$\mathcal{R}_{\rm sr}$ correlation? Though the submm-radio ratio for the local sample decreases by ~ 0.25 dex in the log $L_{\rm FIR}$ range 10–12, the effect is diluted as z increases, since one samples wavelengths closer to 100 μm the corresponding decrease at redshifts of 1, 3, and 5 are only 0.15, 0.07, and 0.05, respectively, much less than the dispersions. These decreases are somewhat less than what one may expect from the SED variation as a function of FIR luminosity, since they are compensated by a decrease in radio emission due to self absorption for high-luminosity sources. We consider this effect in greater detail while discussing the radio spectral index. It is well known that the apparent 850 μm brightness of a source of given luminosity decreases slowly because the slope of the dust emission SED compensates for the distance (Blain, Longair, 1996). For a detection sensitivity of 5 mJy at 850 μm, the threshold value of $\log L_{\rm FIR}/L_\odot$ increases from 11.7 to 12 in the redshift interval 0.5–6 [assuming the average observed ratio of S(353 GHz)/FIR and using $q_0 = 0.5$]. On the other hand, for a given detection sensitivity of the radio continuum emission, the threshold FIR luminosity increases faster. For example, taking the detection sensitivity at 1.49 GHz to be 10 μJy, we find that the calculated threshold luminosity based on the well known FIR-radio correlation changes from $\log L_{\rm FIR}/L_\odot = 10.4$ at $z = 0.5$ to 12.5 at $z = 5$. If we require detection at both 850 μm and 1.49 GHz, the higher of the above defines the threshold luminosity. Assuming the effective range of luminosity to be from the threshold to 0.5 dex higher, the relevant logarithmic luminosity intervals for the range $z = 0.5$–3 and 3–6 are about 12–12.5 $L_\odot$ and 12.5–13 $L_\odot$ respectively. From the data of DS-I, we find that the mean dust temperature in the $\log L_{\rm FIR}/L_\odot$ interval of 11.2–12 is 39.5 K. Based on the observed $T_{\rm d}$–$L_{\rm FIR}$ correlation, the extrapolated temperatures are 42.4 and 44.6 K for the two luminosity intervals above 12. We, then, compute corrections to the $S[353(1+z)\,{\rm GHz}]/S(1.49\,{\rm GHz})$ ratio based on the changes in the ratios of $S[353(1+z)]$/FIR computed using the temperatures for the relevant luminosity interval and an emissivity index of 1.3. It may be noted that the application of the correction for the radio continuum SED transforms the above ratio to $\mathcal{R}_{\rm sr}$, the rest system submm-to-radio continuum FD ratio. The corrected values are lower compared to the values determined from the DS-I data for the 11.2–12 interval. The corrections are 0.23, 0.2, and 0.15 dex at $z = 0.5$, 3, and 6, respectively. It may be noted that the correction decreases for larger z because one is sampling wavelengths closer to 100 μm.

2.2. Radio Spectral Index

In order to compute the expected radio continuum emission at frequencies higher than 1.49 GHz we need

a knowledge of both the FD at $z \approx 0$ and the radio spectral index. CY assumed a spectral index of -0.8. In order to take into account the self absorption at frequencies close to 1.49 GHz, Barger et al. (2000) estimated the FD at 1.49 GHz by extrapolating the observed FD for Arp 220 at a high frequency of 8.4 GHz using a spectral index of -0.8 and using the same index for computing FD at intermediate frequencies. It is true that the observed 1.49 GHz FD is reduced due to self-absorption effect, especially for luminous sources, thus increasing the value of $\mathcal{R}_{\rm sr}$. However, it should be noted that when a distant source is observed, what we measure is not the intrinsic flux, but the emergent flux including the effect of self absorption. Therefore, it is more appropriate to use the observed 1.49 GHz values and make a correction to the expected behavior while computing the submm–radio spectral index as a function of z. Using the available radio data (1.49 GHz: Condon et al. 1990; 4.85 GHz: Condon & Broderick, 1991; Condon et al. 1995), we find the mean and dispersion of the 4.85–1.49 GHz spectral index for the available DS-I sources to be -0.65 and 0.26 respectively. For 21 DS-I sources for which 8.44 GHz data are available (Condon et al. 1991) the 1.49–8.44 GHz spectral index is -0.47. These galaxies have $\log L_{\rm FIR}/L_\odot$ greater than 11. Stine (1992) finds, for a sample of 23 Markarian galaxies, the 1.4–5 GHz spectral index to be -0.64. From these data it is clear that the absorption effect at low frequencies is present. Condon et al. (1991) observed a sample of 40 ultraluminous infrared galaxies, and found that the FIR-to-1.49 GHz radio continuum ratio for luminous ($\log L_{\rm FIR}/L_\odot > 11.4$) sources containing compact radio cores is 0.25 dex higher than that for the rest of the galaxies, which have the standard ratio. When they correct for the self absorption at 1.49 GHz using the 8.44 GHz FD and assuming the real radio spectral index to be -0.7, the corrected mean ratio is normal. If we assume that the self absorption effect is confined to $\nu < 5$ GHz, the spectral index in the 1.49–5 GHz range is then ≈ -0.3. In the DS-I data we also find the effect of self absorption in the FIR to radio continuum ratio. The 4.7–1.4 GHz spectral index of Arp 220 (Anantharamaiah et al. 2000) is -0.3. Taking all the above into account, a reasonable approximation for the radio spectral index would be -0.4 in the 1.49–5 GHz range and -0.7 for frequencies higher than 5 GHz and to scale FDs from the value at 1.49 GHz. Using this approximation and the method enumerated earlier for computing the $S[353(1+z)\ {\rm GHz}]/S(1.49\ {\rm GHz})$ ratio, we calculate $\mathcal{R}_{\rm sr}$ as a function of z using equation 1.

2.3. Relationship between Redshift and Submm-Radio Flux Ratio

The 353–1.49 GHz spectral index computed from this is shown in figure 1 as a solid line. For estimating the dispersion, we use the computed dispersion in the $S[353(1+z)]/S(1.49)$ ratio and also assume $\delta\alpha_{\rm r} = 0.2$. The dispersion of the spectral index is between 0.1 and 0.11. The upper and lower envelopes are shown as dashed lines in figure 1. Our values of the ratio $S[353(1+z)]/S(1.49)$ agree within 0.1 dex with those obtained by Barger et al. (2000) based on the SED and FD of Arp 220; for $z < 1$, our values are lower and for higher z, larger. However, after the application of radio spectral index effects, our 353–1.49 spectral index values are about 0.05 lower throughout. At $z \approx 0$, our index is higher reflecting the free–free absorption effect. It may be noted that our result is not based on a single prototype, but on the data of over 20 galaxies with $\log L_{\rm FIR}/L_\odot > 11.2$.

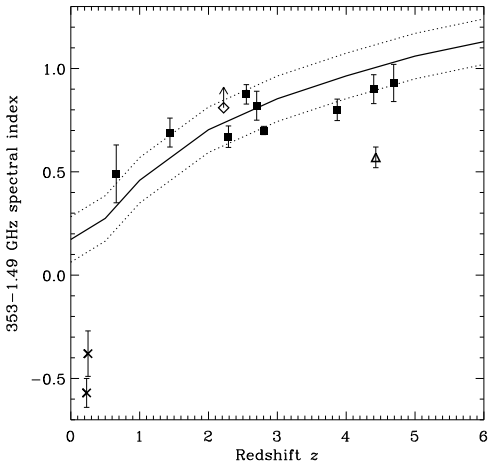

Fig. 1 — The 353 GHz-to-1.49 GHz spectral index, γ, plotted as a function of galaxy redshift, z. The solid line is the computed line and the two dashed lines are the envelopes of dispersion (see text for details). Symbols: filled squares – both γ and z definite; open diamonds – z certain, but radio FD upper limit; crosses – cD galaxies; open triangle – a dusty QSO BRI $0952-0115$. For references to objects and data, refer to subsection 3.1 of the main text.

3. Discussion

3.1. Comparison with Observations

In figure 1 we also show the data points of individual high-z sources compiled from available publications. We have included only well-identified sources that have definite redshift measurements from the near-infrared or CO spectral lines. The objects with the values of redshift in parentheses and references to them are: IRAS F10214+0724 (2.29) (Rowan-Robinson et al. 1993); HR 10 (1.44) (Cimatti et al. 1998; Dey et al. 1999); CFRS 14F (0.66) (Lilly et al. 1999); BR $1202-0725$

(4.69) (Isaak et al. 1994); SMM J14011 + 0252 (2.55) (Ivison et al. 2000); SMM J02399 − 0136 (2.8) (Ivison et al. 1998); APM 08279 + 5225 (3.87) (Lewis et al. 1998); SMM J21536 + 1741 (0.23), SMM J14010 + 0252 (0.25) (Edge et al. 1999); SMM J14010 + 0253 (2.22) (Ivison et al. 2000); LBQS 1230 − 1627B (2.7), BRI 1335 − 0417 (4.4), BRI 0952 − 0115 (4.43) (Yun et al. 2000). We have included CFRS 14F, since Lilly et al. (1999) consider it to be their most secure identification and SMM J14010 + 0253 based on the spectral line identification of Ivison et al. (2000). The 1.4 GHz FD for CFRS 14F has been extrapolated from the 5 GHz FD assuming a spectral index of −0.7. For HR 10, we have used the FDs listed by Dey et al. (1999); the 1.4 GHz FD has been extrapolated from the 3.6 cm measurement. It may be noted that for the three dusty QSOs of Yun et al. (2000) the index is an extrapolation from the 240 GHz measurement assuming a 350–250 GHz spectral index of −3.5. For their fourth source, BR 1202 − 0725, we used the 350 GHz flux density measured by Isaak et al. (1994). The two Edge et al. (1999) sources are cD galaxies in the centers of rich clusters of galaxies, A 1835 and A 2390.

The curve shown in figure 1 is representative of the mean for a sample of galaxies at different redshifts. Individual galaxies may deviate from the curve. An inspection of figure 1 shows that the observed data points populate the region delineated by our calculations. The exceptions are the two cD galaxies and the dusty QSO, BRI 0952 − 0115, which are well below the predicted range. These sources must be dominated by AGN radio emission. It is interesting that for this sample of well-identified sources, there is none occurring above the predicted error zone. We also note that the AGN-dominated sources seem to be clearly separated from the starburst galaxies.

What are the types of sources that may populate regions above the predicted zone? The submm SED may be significantly affected by the presence of cold dust. From ISO observations of a sample of 'active' and 'inactive' galaxies covering a luminosity range of $\log L_{\rm FIR}/L_{\odot} =$ 10–11.2, Siebenmorgen, Krügel and Chini (1999) conclude that while the SED of the former sample is well fitted by a modified blackbody spectrum with a single temperature of ∼ 30–32 K, the latter 'inactive' sample requires the presence of an additional colder component ($T = 11$–16 K). These galaxies have a higher submm-to-FIR flux ratio, and will yield a 353 GHz–1.4 GHz index higher by up to 0.3 as compared to our calculation. From an analysis of their data, we find that the redshift estimate will be most affected at wavelengths close to 850 μm ($z < 1$–1.5) for such galaxies. Such effects may explain the discrepancy between the redshift estimates using the submm–FIR photometric ratio and the submm-radio index for FIRBACK sources of Scott et al. (2000). 'Inactive' galaxies with cold dust may be a significant fraction of the low-z population, and hence an estimate of the redshift from the submm–radio index could distort the picture of the star-formation rate at low redshifts. On the other hand, it is unlikely that such sources are present at high redshifts, since we do not expect very luminous 'inactive' galaxies.

It is of interest to see what is the median redshift of the complete Smail et al. (2000) sample of galaxies. If we use the spectroscopic redshifts for 5 galaxies with reliable identification and estimate the redshift for the remaining 11 galaxies from our submm–radio index curve, we find the median redshift to be ∼ 2.1. In the above, if the estimate is a lower limit, the source is assumed to be at that redshift value. If, on the other hand, we use only the estimated redshift from the submm-radio index and exclude the two cD galaxies, the median redshift is ∼ 2.2. These values are similar to those deduced by Smail et al. (2000) within the error of $\Delta z \sim 1$ at these redshifts.

What are the systematic effects one would expect at higher redshifts? As remarked earlier, higher z sources end to be more luminous, have a steeper FIR–submm SED, and hence, lower 353–1.49 GHz spectral index. If sources with high temperature ($T > 50$ K with $n = 1.3$) are present, they would populate regions lower than the predicted curve. However, there are other effects which may compensate this. If the free–free absorption is high, the radio continuum FD, even at higher frequencies, could be lower, thus increasing the observed 353–1.49 GHz index. Another effect could arise if the emission at 100 μm is optically thick. Solomon et al. (1997), who observed a sample of very high luminosity sources out to redshift of 0.3 in the CO line, conclude that τ_{100} is high for these sources. If the 100 μm optical depth is large, say ≈ 1, the emission can still be optically thin at submm wavelengths, thus increasing the submm–FIR ratio. For an SED characterized by an emissivity index, $n = 1$, and temperature range of 45–55 K, the change in the logarithmic ratio of $S(\nu)$/FIR for the cases $\tau_{100} = 1$ and $\tau_{100} \ll 1$ are increases of 0.17 to 0.24 as the wavelength changes from 200 to 600 μm. These are about the same as the decrease in the individual ratio for $\tau_{100} \ll 1$ while the temperature changes from 45 to 55 K. The presence of an AGN core would also depress the observed ratio. This aspect has been discussed in detail by CY.

3.2. Accuracy of Redshift Estimate

If we want to estimate the redshift from the value of the ratio of submm-to-radio continuum FDs, the uncertainty in redshift is given by the intersection of a horizontal line at that value with the dispersion envelopes shown in figure 1. We, then, find the uncertainties in the redshift estimate at $z = 1, 2, 3, 4$, and 5 to be $\pm 0.33, (+0.7, -0.5), (+0.9, -0.8), (+1.1, -1)$, and ± 1.2, respectively. These uncertainties do not include the

systematic effects discussed in the previous section. At $z \lesssim 2$, the redshift estimate would be reasonably accurate. However, the changes in SED of the source affect the result more than in the high-z region, since the sampled wavelengths are closer to 850 μm. If there is a cold dust component present, the observed spectral index would be higher than the predicted value, and less if the temperature is high. The effects of the SED variation are less for high z, but the flattening gradient gives rise to larger errors. An additional problem is the effect of the large τ_{100} if the sources are very luminous and compact. At $z \gtrsim 3$, the lower limit is perhaps the best result. For $z > 7$, the sensitivity of the technique would be very poor, since the sampled wavelengths are in the flat peak region of the SED. In summary, the 353–1.49 GHz ratio can lead to a crude estimate of a redshift and reasonable lower limits. Hence at present, the study of the distribution of redshifts from just this ratio is premature. The situation will perhaps improve once a larger sample of well-identified galaxies is available and with better knowledge of the systematic effects.

3.3. Photometric Redshift

Hughes et al. (1998) have suggested that the redshift can be estimated from the ratio of FDs in two or more submm bands. For this technique to work, at least one rest system wavelength should be $\lesssim 200$ μm, away from the single power-law region. Scott et al. (2000) have also used the FIR-to-submm FD ratio for their FIRBACK sample. The uncertainties arising from variations in SED will be similar to the submm–radio index method. Unlike the latter method that uses only one rest wavelength sampling, the steep part of the SED, the requirement of measurements at two bands, at least one rest wavelength away from this steep region, reduces the sensitivity of the photometric method. For rest wavelengths > 1000 μm, significant contamination from the thermal free–free emission may be present. This method can be a useful supplement to the submm–radio index method, especially for a redshift range of 1–3.

3.4. Redshift from the Peak of SED

Blain (1999a, 1999b) has suggested that the redshift could be estimated by locating the peak of the dust emission SED. This technique works if all sources are characterized by a constant temperature. Uncertainty in redshift is directly proportional to the changes in the peak wavelength that depends on T, the emissivity index, and the optical depth near the peak. Another factor affecting the redshift estimate is the accuracy with which peak frequency can be located. Apart from the observational constraints arising from the availability of suitable bands for measurement, uncertainty is also introduced by the flatness of the SED in the peak region. We estimate that the resulting error in z is ~ 0.3 at $z = 1$ and ~ 0.9 at $z = 5$. The uncertainty in SED parameters would further increase the errors. If multiband photometry on both sides of the peak are available, a template SED can be fitted to get better accuracy.

4. Conclusions

We have re-examined the method for estimating the redshifts of galaxies using the submm–radio spectral index. For this purpose, we made use of the properties of the 850 μm sample of galaxies observed by Dunne et al. (2000). We compute the variation of the 350–1.4 GHz spectral index as a function of z taking into account the effects of luminosity on the SED and free–free absorption effects on the radio emission. We find that all well-identified sources have their spectral indices either within the error zone, or much lower. The latter, presumably radio-loud AGNs, are well separated from the rest. We also find the median redshift to be ~ 2, which is consistent with that deduced by Smail et al. (2000) within an error of $\Delta z \sim 1$ at these redshifts.

TNR thanks the Japan Society for the Promotion of Science for the award of an Invitation Fellowship and Dr. Hiroshi Shibai for his hospitality.

References

Anantharamaiah, K. R., Viallefond, F., Mohan, N. R., Goss, W, M., & Zhao, J. H. 2000, ApJ, 537, 613
Barger, A. J., Cowie, L. L., & Richards, E. A. 2000, AJ, 119, 2092
Bertoldi, F., Carilli, C. L., Menten, K. M., Owen, F., Dey, A., Gueth, F., Graham, J. R., Kreysa, E. et al. 2000, A&A, 360, 92
Blain, A. W. 1999a, MNRAS, 309, 955
Blain, A. W. 1999b, in Weyman, R.J., Storrie-Lombardi L., Sawicki M., Brunner R. ed., ASP Conf. Ser. 191, Photometric Redshifts and High Redshift Galaxies, 255
Blain, A. W., & Longair, M. S. 1996, MNRAS, 279, 847
Carilli, C. L., & Yun, M. S. 1999, ApJ, 513, L13 (CY)
Carilli, C. L., & Yun, M. S. 2000a, ApJ, 530, 618
Carilli, C. L., & Yun, M. S. 2000b, ApJ, 539, 1024 (erratum)
Cimatti, A., Andreani, P., Rottgering, H., & Tilnaus, R. 1998, Nature, 392, 895
Condon, J. J. 1992, ARA&A, 30, 575
Condon, J. J., Anderson, E., & Broderick, J. J. 1995, AJ, 109, 2318
Condon, J. J., & Broderick, J. J. 1991, AJ, 102, 1663
Condon, J. J., Helou, G., Sanders, D. B., & Soifer, B. T. 1990, ApJS, 73, 359
Condon, J. J., Helou, G., Sanders, D. B., & Soifer, B. T. 1996, ApJS, 103, 81
Condon, J. J., Huang, Z.-P., Yin, Q. F., & Thuan, T. X. 1991, ApJ, 378, 65

Dey, A., Graham, J. R., Ivison, R. J., Smail. I., Wright, G. S., & Liu, M. C. 1999, ApJ, 519, 610
Dunne, L., Eales, S., Edmunds, M., Ivison, R., Alexander, P., & Clements, D. L. 2000, MNRAS, 315, 115 (DS-I)
Edge, A. C., Ivision, R. J., Smail, I., Blain, A. W., & Kneib, J.-P. 1999, MNRAS, 306, 599
Helou, G., Khan, I. R., Malek, L., & Boehmer, L. 1988, ApJS, 68, 151
Hughes, D. H., Serjeant, S., Dunlop, J., Rowan-Robinson, M., Blain, A., Mann, R. G., Ivison, R., Peacock, J., et al. 1998, Nature, 394, 241
Isaak, K. G., McMahon, R. G., Hills, R. E., & Withington, S. 1994, MNRAS, 269, L28
Ivison, R. J., Smail, I., Barger, A. J., Kneib, J.-P., Blain, A. W., Owen, F. N., Kerr, T. H., & Cowie, L. L. 2000, MNRAS, 315, 209
Ivison, R. J., Smail, I., Le Borgne, J. -F., Blain, A. W., Kneib, J.-P., Bezecourt, J., Kerr, T. H., & Davies, J. K. 1998, MNRAS, 298, 583
Lewis, G. F. Chapman, S. C., Ibata, R. A., Irwin, M. J., & Totten, E. J. 1998, ApJ, 505, L1
Lilly, S.J., Eales, S. A., Gear, W. K. P., Hammer, F., Le Fèvre, O., Crampton, D., Bond, J. R., & Dunne, L. 1999, ApJ, 518, 641
Rowan-Robinson, M., Eftasthiou, A., Lawrence, A., Oliver, S., Taylor, A., Broadhurst, T. J., McMahon, R. G., Benn C. R., et al. 1993, MNRAS, 261, 513
Scott, D., Lagache, G., Borys, C., Chapman, S. C., Halpern, M., Sajina, A., Ciliegi, P., Clements, D. L., et al. 2000, A&A, 357, L5
Siebenmorgen, R., Krügel, E., & Chini, R. 1999, A&A, 351, 495
Smail, I., Ivison, R. J., Owen, F. N., Blain, A. W., & Kneib, J.-P. 2000, ApJ, 528, 612
Soifer, B. T., Boehmer, L., Neugebauer, G., & Sanders, D. B. 1989, AJ, 98, 766
Solomon, P. M., Downes, D., Radford, S. J. E., & Barrett, J. W. 1997, ApJ, 478, 144
Stine, P. C. 1992, ApJS, 81, 49
Yun, M .S., Carilli, C. L., Kawabe, R., Tutui, Y., Kohno, K., & Ohta, K. 2000, ApJ, 528, 171